Electron capture into eight excited states of ^{7}Li in collisions of 2-keV ^{7}Li$^+$ on H$_2$

Benjamin L. Blaney* and R. Stephen Berry

*The University of Chicago, Department of Chemistry, Chicago, Illinois 60637*

We have measured relative intensities of emission from the $2p$, $3s$, $3p$, $3d$, $4s$, $4d$, $5s$, and $5d$ states of ^{7}Li produced in 444-eV (relative energy) collisions (2-keV ions on thermal molecules) of ^{7}Li$^+$ with H$_2$. From these, relative values of the direct charge-transfer cross sections σ_c were obtained. It was found that σ_c decreases rapidly and smoothly (approximately as $10^{-(n-3)}$), with increasing principal quantum number n (for $n = 3$, 4, 5) while the variation in σ_c with angular momentum quantum number is not regular; $\sigma_c(3s) \sim \sigma_c(3p)$ but $\sigma_c(nd) \sim 10\sigma_c(ns)$, in sharp contrast to the behavior of capture cross sections at high energies.

INTRODUCTION

Electron capture by the ion in ion–diatomic-molecule collisions may be denoted by the general equation

$$A^+ + BC \xrightarrow{\sigma_c(nl)} A^*(n,l) + \cdots ,$$
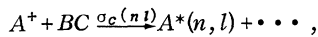
where n and l are the principal and angular momentum quantum numbers of the A^* electronic state, and where the cross section for direct charge transfer into that state is $\sigma_c(nl)$. For sufficiently rarefied reaction systems, the rate of formation of A^* may be monitored directly by observing emission due to radiative decay.

Considerable effort has been expended in investigating the simplest such reaction, $H^+ + H_2$ (cf. Hess[1] and Thomas[2] and references listed therein). Interest in this system derives primarily from the relative simplicity of theoretical calculations involving capture into electronic states of the hydrogen atom. Studies at high energies (> 10 keV) indicate a distinct variation of σ_c with both n and l quantum numbers.[3] However, the dependence of σ_c on l is difficult to obtain from these experiments because of the degeneracy of the l quantum levels in any particular n quantum state of H. Comparison of the work of Hughes and co-workers with that of Ford and Thomas[4] at high energies shows discrepancies in their experimentally determined values of $\sigma_c(nl)$ as large as a factor of 5 at 100 keV projectile energy (laboratory system, with target at rest). (All unspecified collision energies in this article refer to the laboratory frame energy of the ion beam. The target gas is essentially at rest.) They employ similar experimental techniques, differentiating states *of different lifetimes* which contribute a given Balmer line by monitoring the emission intensities as functions of distance behind a thin interaction region. Recently Hess[1] used a different experimental approach to measure $\sigma_c(n)$ ($n = 3, 4$) at energies of 0.3–3.0 keV. Because he monitors the emission in the interaction region,

Hess cannot determine σ_c for individual l. But since $\sigma_c(n) = \sum_l \sigma_c(nl)$, we may compare the results of the two experimental techniques. If one extrapolates Hess's data to 10 keV, we find that his value of $\sigma_c(n)$ is only one-fourth of the sum of the partial cross sections of Hughes *et al.*, well outside the limits of uncertainty claimed by these authors.

An alternative approach to elucidating the dependence of σ_c on l quantum number is the investigation of a system whose excited atomic energy levels are sufficiently split to allow spectroscopic resolution of emission from different l states while preserving the hydrogenic nature of the orbitals as much as possible to simplify the work of the theoretician. For this reason, we chose to investigate collisions of ^{7}Li$^+$ on H$_2$. An energy-level diagram of LiI indicating the monitored emission wavelength is shown in Fig. 1. In the experiments reported here, we restrict our investigation to a single-projectile collision energy of 2.00 keV corresponding to a collision velocity of 2.3×10^7 cm sec^{-1} and a center-of-mass energy of 444 eV.

The high luminous flux collection efficiency of our system permitted detection of processes with low cross sections (estimated to range from 2×10^{-18} to $\sim 10^{-21}$ cm^2), even at low ($\lesssim 10^{-4}$ Torr) target pressures. It is possible to make an order-of-magnitude estimate of the absolute value of our capture cross sections from the following considerations:

We find that the intensities of the atomic lines produced in 2-keV collisions of Li$^+$ on H$_2$ are, to within 30%, a factor of 30 lower than in collisions with N$_2$. Neff[5] reports a value of $2–4 \times 10^{-17}$ cm^2 for the $\lambda 670.8$ emission cross section in Li$^+$-N$_2$ collisions at 1 keV. Extrapolating this value to 2 keV and assuming cascade contributions to be small, we estimate the $\sigma_c(2p)$ to be $5 \pm 2 \times 10^{-17}$ cm^2 for a nitrogen target and $2 \pm 1 \times 10^{-18}$ cm^2 for Li$^+$ on H$_2$ and $\sigma_c(5s)$ to be of order or less than 2×10^{-21} cm^2.

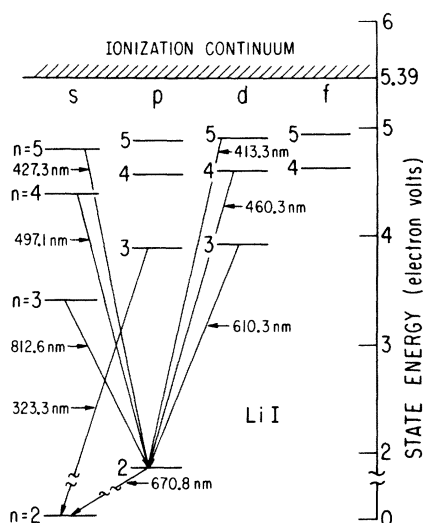Some alkali-ion–molecule (or atom) electron-

FIG. 1. Partial energy level of Li I. Energies of excited states above ground state Li (2s) are scaled to ordinate. Monitored transitions are shown by lines connecting initial and final states. The emission wavelength associated with each transition is given in nm.

FIG. 2. Top-view schematic representation of apparatus. See text for details.

capture experiments in the low-keV energy range have been reported previously.[2,6–8] Neff has also done a large amount of unpublished work, much of it in conjunction with Tolk.[5] All of these studies involve collisions of alkali ions with N$_2$, O$_2$, and He and none quantitatively determines the charge capture cross sections for as many excited states in a single system as are reported here.

APPARATUS

The apparatus consists of a mass-analyzed beam of ^{7}Li$^+$ passing through a chamber of hydrogen gas and a photon detection system whose field of view intersects the beam at right angles to its trajectory. Figure 2 is a top view schematic of the chamber showing tungsten mesh surface-ionization ion
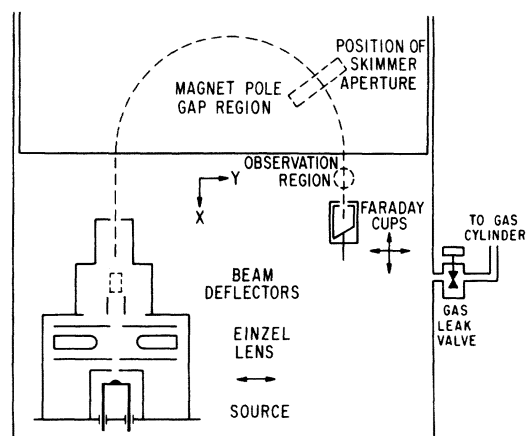
source, electrostatic ion optics, 180° sector magnet, and current monitoring Faraday cups. These components and the single vacuum chamber in which they are enclosed have been described in detail earlier.[9,10] Figure 2 shows the position of the observation region located 8.5 cm from the pole face of the magnet. The axis of the detection optics enters the chamber through a $\frac{3}{16}$-in.-thick quartz window (see below) and has a field of view whose diameter is approximately 1.0 cm in the region of the ion beam. Typically the beam cross section is 0.8 cm square at the observation region. The well-defined verticle beam profile results from passing the beam through an aperture inside the magnet which skims off the diverging upper and lower ion extremities. Sharp profiles are obtained in the horizontal plane by proper electrostatic focusing.

Linde research grade H$_2$ gas (99.995% purity) is admitted to the chamber through a Granville Phillips variable leak valve. Pressures in the liquid-nitrogen–trapped, diffusion-pumped chamber
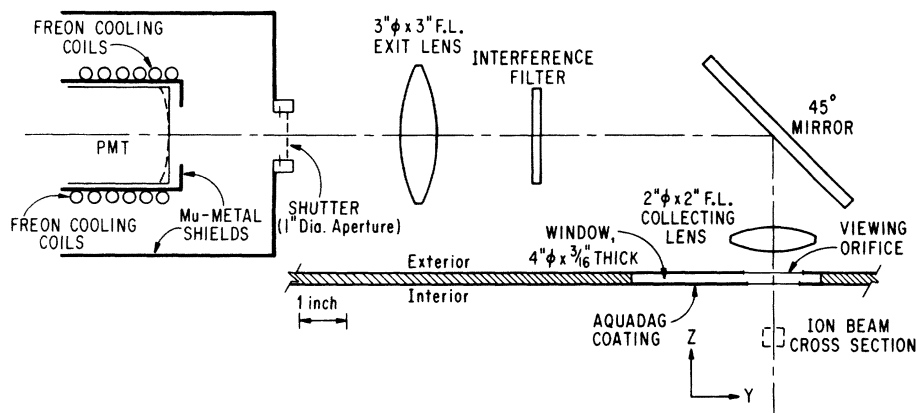

FIG. 3. "Periscope optics" light-collection system viewed from main chamber, looking towards the bending chamber. The trajectory of the ion beam as it exits the magnet is perpendicular to the page. Only two of the four μ-metal PMT shields are shown. See text for further details.

are measured with a General Electric nude ionization gauge tube and a Granville Phillips controller.

Figure 3 presents the "periscope optics" light-collection system which rests on top of the chamber, immediately adjacent to the pole face of the magnet. An Aquadag (graphite colloid) coating shields the optics from stray light in the chamber. The cross section of the ion beam as it proceeds away from the magnet is shown below this window. The periscope optics consists of two quartz lenses (Esco Optics, Inc.), an aluminum front surface mirror, an interference filter of the desired band-pass, and a photomultiplier tube (PMT) encased in four μ-metal shields. Prototypes of RCA 8850 and 8852 tubes were employed giving a spectral range of 300 to 850 nm with dark counts of 50 and 90 Hz, respectively. In the latter case the tube is cooled to $-25°$ C by a freon refrigeration system. Both lenses have $f/1$ apertures. The focal plane of the 3-in.-diam exit lens lies at the shuttered aperture to the PMT housing; the focal plane of the 2-in.-diam collecting lens lies in the horizontal midplane of the ion beam.

Various 2-in.-square, narrow-band dielectric interference filters (Corion Instrument Corp. and Ditric Optics, Inc.) were used to monitor emission lines and background. Bandwidths at half-maximum transmission ranged from 3.2 to 11.5 nm. Filters were chosen with maximum transmission near the particular atomic emission line of interest. Provision was made for tilting the filters up to 20 deg with respect to the optical axis of the detection system. The resultant shift in bandpass effectively blocked the emission line and allowed the measurement of the background continuum.

The optical system was designed so that detected photons are diverging from the optical axis by at most 10° in the region where they traverse the interference filter. This was done in an attempt to insure a low distortion of filter bandpass over the cross section of the light beam. Despite this precaution it was found that calibration of the filters at different tilt angles using a standard spectrophotometer (e.g., Cary 14) was unreliable. In particular, these measurements did not replicate the results obtained when the filters were tilted *in situ* to transmit collision-induced atomic lines. These lines were produced by ion-atom collisions, e.g., Na$^+$ and Ar at selected wavelengths where no target gas emission was present [e.g., Na (λ330.4)]. A cylindrical light source made of a 3–4-mm-diam × 3-cm-long quartz rod with roughened surfaces and illuminated with light from a Jarrell-Ash 0.25-m monochromator have transmission data which was reliable to within 15%.[11]

The single-photon counting electronics have been described previously[9] and the details of their calibration are presented in the Appendix. The uncertainty of the relative counting efficiencies was determined to be $\lesssim 10\%$, arising principally from the uncertainty in detection efficiency of a Coherent Radiation Model 212 flux meter.

Polarization of the emitted signal was not measured and the effects of "instrumental polarization" were not determined. The former is generally small ($\lesssim 20\%$) with the result that the maximum uncertainty in the cross section may be calculated, using standard equations,[2] to within an uncertainty of $\lesssim 6\%$. One would expect the prime contributors to instrumental polarization to be the tilted interference filters and the 45° mirror. It has been shown that the effects of polarization on transmission of dielectric interference filters are negligible for angles of tilt $\lesssim 20°$.[12] This fact determined the upper limit of filter tilt in our experiments.

Variation of the mirror reflectance components R_s and R_p at 45° from those for normally incident light, $R(0°)$, are expected to be small and symmetrical $[(R_s - R) \sim (R - R_p)]$ throughout the spectral range because at all wavelengths the sum of the square of the index of refraction and coefficient of absorption is $\gg 1$.[13] Therefore the net reflectance $R(45°) = \frac{1}{2}[R_s(45°) + R_p(45°)] \sim R(0°)$. The reflectance at normal incidence is approximately 90% for typical aluminum mirrors throughout the visible and drops appreciably only below 400 nm.[14] The reflectance of our mirror at 320 nm was taken to be $80 \pm 5\%$ and the corresponding correction was included in the analysis of the experimental data.

DATA ACQUISITION

Under typical operating conditions the magnetic field was 2300 G and the residual chamber pressure was less than 2×10^{-7} Torr. Maximum ion current and density in the observation region were 3 μA and 10^6 cm^{-3}, respectively. Hydrogen pressures ranged from 10^{-5} to 2×10^{-4} Torr. Collisional depletion of the ion beam current was negligible.

The intensities of emission from lithium lines spanned a wide range, varying with the initial energy level, the spectral dependence of the efficiency of the photon collection system, the H$_2$ pressure, and the intensity of the ion beam. For the $2p \rightarrow 2s$ transition, count rates were as high as 400 kHz. In almost all cases, the count rate from lithium emission was at least 84% of the total. The only exceptions were emissions originating in the $n = 5$ states where signal strengths were sometimes only twice the background emission. The nearby H$_\gamma$ and H$_\delta$ lines, though apparently weak, also complicated the analysis near 400 nm. Because of the large ($\sim 50\%$) uncertainties in the relative atomic and background contributions, the re-

ported cross sections for the $n = 5$ states are given as upper limits to the capture cross sections.

Besides lithium atomic emission, the monitored count rates also included beam–residual-gas and beam-chamber interactions, continuous background light sources, and diffuse H_2 emission. By counting with no H_2 in the chamber, the contribution from the former two was obtained. The residual-gas and chamber interaction signals were 3%, or less that of any particular Li signal emission line. The principal continuous light source was the ion beam source. With optical shielding, the contributions from this signal produced quite stable count rates of ~ 700 ± 15 Hz at 820 nm and 50–100 ± 15 Hz for $\lambda < 600$ nm. The intensity of the H_2 emission passing through each filter was obtained by counting photons after tilting the filter to shift its bandpass until the atomic emission line was blocked. Molecular hydrogen emission signals were typically ~ 20–50 Hz over a bandpass of ~ 10 nm.

The intensity of molecular hydrogen emission in the neighborhood of the various lithium lines was monitored at wavelengths 10–15 nm away from the alkali lines. To estimate the contribution of H_2 emission to the count rate at the alkali line frequencies, we assumed that the molecular emission is a smooth function of frequency in the vicinity of each line. This was consistent with our observation that the background near each line varied, as function of the filter tilt angle, in direct proportion to the transmittance of the filter. With the exception of emission in the region of the $n = 5$ levels, the emission from H_2 was weak, usually a factor of 100 smaller than the Li emission. We also note that Andreev, Ankudinov, and Bobashev have monitored emission in the visible-light region due to collisions of He^+ and Ne^+ with H_2, at laboratory energies of 5–35 keV.[15] They observed the first five Balmer lines but found no H_2 emission. The smallest cross section they report, for H_ϵ, is about 2×10^{-20} cm^2 with Ne^+ at the

lowest energy, corresponding to an ion velocity of 3×10^7 cm/sec. The emission cross sections from Ne^+ increase with beam energy; with He^+, they are of the same magnitude but are approximately independent of energy in this region. The Balmer cross sections measured by Andreev et al. are of the same magnitude as the analogous cross sections we observe for capture by Li^+ in our experiment. We infer from our own measurements and those of Andreev et al. that our procedure for correcting for H_2 emission is adequate, within the accuracy of our experiments except perhaps for the $n = 5$ levels, where we claim only to have set upper bounds on the cross sections.

An experimental run consisted of measuring the signal count rate at base chamber pressures with the $\lambda 610.3$-Å transmitting filter and then with a filter transmitting the emission line of interest. Counts were taken both with the filters normal and tilted with respect to the detector optical axis. Hydrogen was then admitted to the chamber and the filter tilting procedure was repeated. Total ion beam currents were measured before and after each change in filter angle. (The Faraday cup was moved out of the beam path during photon counting.)

By taking into account the variation in detector collection efficiency and integral transmittance of each filter with angle of filter tilt, relative emission intensities with respect to any emission line could be obtained. We report intensities relative to the Li ($\lambda 670.8$) line, $N(\lambda)/N(670.8)$. These results are presented in column 3 of Table I. Because of the close proximity of two Balmer lines to the lithium emission lines corresponding to $5s \rightarrow 2p$ and $5d \rightarrow 2p$ transitions, it was possible only to obtain an upper limit to the relative emission intensities of these two $n = 5$ states.

DETERMINATION OF DIRECT CHARGE-TRANSFER CROSS SECTIONS AND CASCADE CONTRIBUTIONS

In order to determine the direct charge-transfer cross sections involved in Li^+-H_2 collisions a

TABLE I. Relative emission strengths and direct charge-transfer cross sections.

Transition	n	Wavelength (nm)	$N(\lambda)/N(6708)$	$\sigma_c(j)/\sigma_c(2p)$
$ns \rightarrow 2p$	3	812.6	0.023 ± 0.005	$1.9 \pm 0.9 \times 10^{-2}$
	4	497.2	$1.1 \pm 0.2 \times 10^{-3}$	$1.9 \pm 0.7 \times 10^{-3}$
	5	427.3	$< 2 \times 10^{-4}$	$< 4 \times 10^{-4}$
$np \rightarrow 2s$	2	670.8	$\equiv 1.0$	$\equiv 1.0$
	3	323.2	$3.1 \pm 0.5 \times 10^{-3}$	$2.3 \pm 0.9 \times 10^{-2}$
$nd \rightarrow 2p$	3	610.3	0.15 ± 0.02	$1.4 \pm 0.4 \times 10^{-1}$
	4	460.3	0.017 ± 0.003	$2.5 \pm 0.6 \times 10^{-2}$
	5	413.3	$< 8 \times 10^{-4}$	$< 1 \times 10^{-3}$

model was developed which related the populations per unit length $n_x(j)$ of any state j in the interaction region to state-populating mechanisms along our particular beam trajectory (recall that the trajectory is curved until it nears the observation region). Since the experiment was done under single-collision conditions, population occured only by direct charge transfer with cross section $\sigma_c(j)$ or by radiative cascade from higher states, k. From an expression describing the population process, the relative values of $\sigma_c(j)$ could be determined because $n_x(j)/n_x(2p)$ is directly proportional to $N(\lambda)/N(670.8)$. Here $hc/\lambda = E(j) - E(i)$, i being some lower state of the atom to which the radiative decay occurred.

Figure 4 shows the relevant part of the beam trajectory lying between the magnet pole face and the observation region. It is evident that most of the neutrals formed well upstream of the observation region are produced on the curved part of the trajectory and therefore will miss the observation region completely, because they follow straight-line paths from the point of charge capture. Thus the ion trajectory can be divided into two parts, a straight-line trajectory (SLT) region which was taken to extend 5.0 cm in front of the observation region and from which $\gtrsim 95\%$ of the neutrals formed pass through the observation region, and a curved trajectory (CT) region from which only a small fraction of the neutrals reached the observation region. Except in the case of the relatively long-lived $3p$ state it was possible to show that all states whose emissions were observed could only
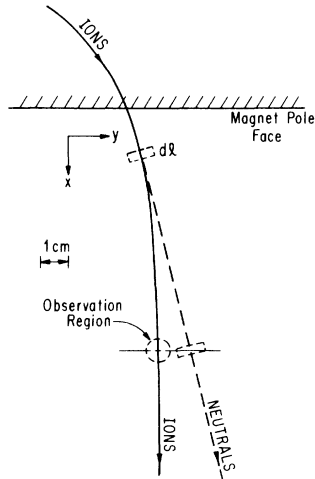

FIG. 4. Ion beam trajectory and typical neutral trajectory near observation region. Dashed trajectory (— —) is that of neutrals formed in infinitesimally small distance, dl. Their trajectory is tangent to ion beam (———) at the point of charge capture.

be significantly populated from processes occurring in the SLT region. This follows from the fact that for our 2-keV beam the transit time of the SLT region is 2.2×10^{-7} sec while the state lifetimes lie between 0.14 and 1.04×10^{-7} sec.[16] Even in the case of the $3p$ state, it could be shown that there was only an 11% contribution from the CT region. The smallness of the contribution from the CT region is important because it could be estimated only to within a factor of 2 and would have generated larger uncertainties in our data had it significantly influenced $n_x(j)$.

Having reduced our problem to one of a straight-line trajectory, we assumed that only single-step cascade processes contributed significantly. We shall see that this approximation is justified by the fact that direct charge-transfer cross sections drop off rapidly with increasing energy of the electronic state and because lifetimes increase with state energy.

Under these assumptions, the variation in state population along the beam trajectory is

$$v\frac{dn_x(j)}{dx} = \frac{I_+}{e}N\sigma_c(j) + \sum_{k>j}A_{kj}n_x(k) - \frac{n_x(j)}{\tau(j)}, \qquad (1)$$

where v is the ion beam velocity, I_+ is the beam current, N is the H_2 density, A_{kj} is the transition probability from state k to state j, and

$$\tau(j) \equiv \left(\sum_{i<j}A_{ji}\right)^{-1}$$

is the lifetime of state j. Transition probabilities and state lifetimes were obtained from tabulations of the National Bureau of Standards.[16] Since states higher then j are assumed populated only by direct change transfer, it follows that

$$n_x(k) = (I_+/e)N\sigma_c(k)\tau(k)\{1 - \exp[-(x-5)/v\tau(k)]\}. \qquad (2)$$

Equation (1) may now be solved analytically to give

$$n_x(j) = \left(\sum_k\frac{\beta(k)}{B(j) - B(k)} - \frac{\gamma(j)}{B(j)}\right)\exp[-B(j)(x-5)]$$

$$-\sum_k\left(\frac{\beta(k)}{B(j) - B(k)}\right)\exp[-B(k)(x-5)] + \frac{\gamma(j)}{B(j)}, \qquad (3)$$

where

$$\beta(k) = \frac{A_{k\to a}K(k)}{vB(k)}, \qquad \gamma(j) = K(j) + \sum_k\frac{A_{k\to j}K(k)}{vB(k)},$$

and for any state

$$K(i) = (I/ev)N\sigma_c(i), \qquad B(i) = [v\tau(i)]^{-1}.$$

In a more detailed treatment[11] we included state

populations from the CT region as initial values when integrating over dx and thus were able to verify directly that the contribution of this region to $n_x(j)$ is unimportant.

To obtain quantitative results from expression (3) we restrict ourselves to a finite set of excited states—those with quantum numbers $n \le 5$ and $l \le 3$. All other states were shown to contribute negligibly because of their long lifetimes and/or because, as we shall see, capture cross sections decrease rapidly with increasing n quantum number.

Cross sections were calculated in stages. First, approximate charge-capture cross sections for the observed states were obtained by assuming no cascade contributions to $n_x(j)$. These zeroth-order values $\sigma_c^0(j)$ are close to the final values obtained because in almost all cases cascading is small. From this set, cross sections were estimated for the production of unobserved states by assuming their capture cross sections $\sigma_c(k)$ followed the general trends indicated by the observed states. In particular, the "first-approximation" cross sections $\sigma_c^0(j)$ decreased approximately as $10^{-(n-3)}$ for s and d states. We therefore assumed that the same was true for p and f states. We also found that $\sigma_c^0(nd)/\sigma_c^0(ns) \sim 10 \pm 2$, approximately twice the ratio of statistical weights. Therefore we suppose $\sigma_c^0(nf) \lesssim (2 \times \frac{7}{5})\sigma_c^0(nd)$ or $\lesssim 3\sigma_c^0(nd)$. We feel that this is a reasonable upper limit to $\sigma_c^0(nf)$ based on the following consideration of conservation of angular momentum. The ground-state orbital angular momentum of the electron of H$_2$ (not constant of the motion) is on the order of one unit of $\hbar$. At our relative collision energies only a small amount of angular momentum may be obtained from relative motion of electron and ion. That is to say, $mbv/\hbar \lesssim 1$ for impact parameters $b \lesssim 5$ Å. We conclude that a dropoff in $\sigma_c(a)$ with increasing l must start occurring at states of l quantum number not too much larger than 2 and that therefore $\sigma_c(a)$ should not increase any faster than we observed in considering the s and d states. Having established reasonable upper limits to $\sigma_c^0(nf)$ we took two-thirds these values as most probably cross sections for use in our cascade calculations, realizing that it was very unlikely that $\sigma_c^0(nf) \sim 0$. We expect these values of $\sigma_c^0(nf)$ to have approximately a 50% uncertainty.

We proceeded to calculate the cascade contributions to the monitored states by using the $\sigma_c^0(k)$ values as the transfer cross sections for all of the relevant higher states. Calculations were done in the following order: 4s, 4d, 3d, 3p, 3s, 2p. The resultant relative direct capture cross sections are found in column 4 of Table I. Cascade contributions from states $k > j$ are listed in Table II. Where cascade is negligible (<1%) $\cdots$ appears.

TABLE II. Cascade contributions.

State	States considered for contribution through cascade	Percentage cascade contribution
2p	3s	3 ± 1
	3d	12 ± 6
	4s	$\cdots$
	4d	1 ± 0.3
	5s	$\cdots$
	5d	$\cdots$
3s	3p	36 ± 14
	4p	$\cdots$
	5p	$\cdots$
3p	4s	3 ± 0.5
	4d	17 ± 5
	5s	$\cdots$
	5d	$\lesssim 1$
3d	4p	$\cdots$
	4f	19 ± 10
	5p	$\cdots$
	5f	2 ± 1
4s	5p	$\cdots$
4d	5p	$\cdots$
	5f	4 ± 2
	6f	$\cdots$

The effects of the 50% uncertainties of $\sigma_c^0(nf)$ have been included along with propagated random errors in obtaining the uncertainties of σ_c for monitored states. The result is an additional 15% uncertainty in $\sigma_c(3d)$ and 5% uncertainty in $\sigma_c(4d)$. The effect of the uncertainty of the CT region contribution on the 3p population was conservatively estimated at 6%. These are the only significant contributions which our model adds to the uncertainty of the final result, σ_c. In all other cases, experimental uncertainties predominate.

Clearly our assumption of only single-step cascade processes is justified although this is partially because of the fortuitous values of transition probabilities. The largest two-step cascade affects the 2p population and derives from the $4f \rightarrow 3d$ transition because of the uniquely shorter lifetime of the 3d state relative to the 2p state. There is at most a 4% uncertainty in $\sigma_c(2p)$ because of this process. In all other cases two-step contributions are very small, either because the single-step cascades are weak or, as in the case of the $3p \rightarrow 3s$ transition, the magnitude of the process, relative to the population of the state it will effect, is small [i.e., $\sigma_c(3s) \sim 10^{-1}\sigma_c(2p)$].

DISCUSSION

To date the most extensive theoretical and experimental studies of charge transfer to specific

atomic excited states have involved proton-atom (molecule) collisions above 25 keV where the Born approximation is valid (e.g., Band[17] and Hughes et al.,[3] and references included therein). Although no theoretical work is available for comparison covering the energy of our experiment, some insight may be gained by comparing our results with those of the Born region.

Let us first examine the basis of the rapid decrease in σ_c with principal quantum number. Oppenheimer predicted a decrease in $\sigma_c(ns)$ as n^{-3} for high collision energies.[18] Later Jackson and Schiff[19] noted that this rule could be generalized to predict the variation of $\sigma_c(n)$, the total capture cross section for a given n level. This "rule" is understandable on physical grounds by examining what contributions are important to the charge-transfer amplitude in various energy regions. The principal contributions to the T-matrix elements come normally from internuclear distances at which the electronic overlap is largest between initial- and final-state wave functions. This criterion embodies a propensity toward conservation of momentum of the active electron, insofar as the overlap tends to be largest when the mean local wavelengths of overlapping initial and final one-electron functions are similar.

In low-energy collisions, most of the transition amplitude for charge transfer comes from regions of internuclear distance in which the outermost lobes or even the tails of the electronic wave functions contribute most of the overlap. At higher collision energies, the velocity due to the relative motion of the donor and acceptor has the effect of shortening the de Broglie wavelength of the electron. In collisions of sufficiently high energy, the momentum of the active electron coming from relative motion of the colliding particles shortens that wavelength so much that the maximum overlap of initial and final states occurs when the nuclei are relatively close and the charge transfer occurs between inner parts of the orbitals.[20] The amplitudes of the probability densities of the inner lobes of Coulomb functions fall off as $\sim n^{-3}$, yielding the observed scaling rule. This rule predicts, then, relative magnitudes for σ_c of 1:0.4:0.2 for the $n = 3$, 4, and 5 levels at high collision energies.

Our cross sections, by contrast, fall off more quickly. We infer that the inner, "penetrating" parts of the acceptor orbitals responsible for the n^{-3} scaling rule do not dominate the behavior of the acceptor channel when the relative energy is in our range of a few hundred volts. The lobe of a 1s hydrogenic wave function corresponds to an electron velocity of order 10^8 cm/sec. In the energy range of our experiments only the outer lobes of the 4f and $n \geq 5$ orbitals are broad enough to

yield sizable overlaps with the moving H_2 orbitals. Therefore there is little reason to expect the inner parts of the acceptor orbitals to play important roles at the velocities we used in determining σ_c; collisions with large impact parameters must be making significant contributions and the n^{-3} scaling rule should not apply.

Since the radial probability in the $r < a_0$ of different l states in a given n level falls off with increasing l quantum number, one would expect a decline in $\sigma_c(nl)$ with increasing l. This has been observed in H^+-H_2 collisions at high energies[3,4] and has been obtained from theory for high-energy H^+-H_2 collisions.[17] At proton energies below the lower limit of the Born approximation (i.e., < 25 keV), this simple relation is observed to break down;) in fact Hughes finds that $\sigma_c(3s)$ $\sim \sigma_c(3p) < \sigma_c(3d)$ for $5 < E < 10$ keV. This inversion in l dependence has been explained for proton and other atomic ion collision systems on the basis that the ion velocity in this energy range is comparable to the orbital velocity of the electron.[21] Since electrons in orbitals of high angular momentum are found, on the average, further from the nucleus, their average velocities are smaller and consequently the collison energy of maximum charge-transfer probability is expected to decrease with increasing l. If the magnitudes of the cross sections at their maxima are comparable, as is found experimentally to be the case for H^+-H_2, a dependence of σ_c on l is inverted from that found in the Born limit. We expect that a similar inversion may result for other hydrogenlike systems such as ours; therefore the l dependence of our results appears to be consistent with expectations based on higher-energy behavior.

The increase of capture cross section with angular momentum quantum number also appears to be born out in a qualitative manner by the limited work by other groups on ion-molecule charge capture at collision energies close to ours. Neff has provided us with emission data for Li^+ +N_2, O_2, and CO collisions at 500 eV.[5] He monitored the 2p, 4s, 3d, 4d, and 5d states and calculated total population cross sections. If cascade contributions to state populations are much smaller than direct charge transfer, as our experiment appears to indicate, Neff's total cross sections are approximately equivalent to σ_c. His experiments yield a ratio for the 4d-to-4s cross section ranging from 5 to 10, in qualitative agreement with our results. Harris and co-workers have recently presented relative luminescence intensities from He^+-O_2 collisions at energies up to 400 eV in emission spectra between 194.0 and 850.0 nm.[22] Their maximum collision energy corresponds to a relative collision velocity of approximately one-half of ours. When

one transforms the reported emission intensities into total population cross sections it is found that they are approximately equal for the $3\,^3S$ and $3\,^3P$ states and that the ratio of cross sections of $(3\,^3D, 3\,^3S)$, $(3\,^1D, 3\,^1S)$, and $(4\,^3D, 4\,^3P)$ vary from 4 to 6.5. For both these research groups, then, the s and p levels are populated with approximately equal probability while charge transfer to the d level occurs at a significantly higher rate, in accord with the results observed in our experiments.

For a given l quantum number, the cross sections obtained from the work of both Neff and Harris drops off more rapidly than n^{-3} with increasing principal quantum number, in agreement with our findings. In all cases the absolute value of the slope is at least twice that predicted by the Jackson and Schiff scaling rule. Recently Dawson and Loyd reported cross sections for electron capture into the 3s and 4s states of atomic hydrogen by H^+ and D^+ impact on He, Ar, and Kr.[23] Ion beam energies ranged from 1.2 to 8.2 keV. The lowest velocity in their experiments corresponds to approximately twice that of our work. They find that $\sigma(3s)/\sigma(4s)$ increases with decreasing beam energy, rising to values of 5.4, 5.3, and 9.0 for the respective target atoms at 1.2 keV. The value of $\sigma(3s)/\sigma(4s) = 10$ which we obtain for Li^+ on H_2 appears to be entirely consistent with their results.

ACKNOWLEDGMENTS

APPENDIX: CALIBRATION OF THE PHOTON COLLECTION SYSTEM

Prototypes of RCA 8850 and 8852 photomultiplier tubes were employed to cover the spectral region of interest. For wavelengths of 500–900 nm it was possible to calibrate the tubes absolutely. The spectral variation of the radiant flux from a Jarrell-Ash 0.25-m Ebert monochromator could be measured to within ± 7% with a Coherent Radiation Model 212 fluxmeter. A stable, intense light source at the monochromator entrance slit was provided by a Sylvania FAD tungsten halogen lamp. We measured the radiant flux and then placed the photomultiplier at the monochromator exit slit. Schott glass filters in front of the photomultiplier reduced the flux from the monochromator below the saturation level of the tube. Approximately 75% of the photocathode was illuminated. Since the spectral transmission curves of the filters could be measured with a Cary 14 spectrophotometer, the absolute responsivity of the photon collection system was readily obtained. The spectral irradiance varied by only 2–3% during the course of these measurements. We estimate the uncertainty in relative responsivity at wavelengths above 500 nm to be $\leq 10\%$.

No flux meter of sufficient sensitivity was available for measurements at wavelengths shorter than 500 nm. In that region we used a light source with known spectral distribution and a readily calibrated monochromator. The Sylvania FAD tungsten halogen bulb and various narrow-band interference filters served the purpose. When the lamp was operated at 121 V ac, its irradiance agreed with those of the standard tungsten halogen lamps calibrated by the National Bureau of Standards[24] to within 3%, at the four wavelengths 500, 590, 656, and 800 nm. We then assumed that the NBS curves of irradiance could be used for wavelengths between 400 and 500 nm. With the lamp and suitable neutral-density and narrow-band interference filters we calibrated the 8850 photomultiplier between 400 and 500 nm. Because Schott filters do not transmit appreciably below 400 nm, the relative responsivity of the tube in the region of 323 nm was determined by normalizing the "typical" quantum efficiency curve supplied by RCA to that which we measured in the region of 400 to 620 nm. The uncertainty of the relative responsivity in the region of 400–500 nm is estimated to be on the order of 10%; since typical quantum efficiency curves vary as much as 20% (according to the manufacturer), the uncertainty of the relative responsivity at 323 nm is taken to be 25%.

*Present address: Department of Chemistry, Indiana University, Bloomington, Ind. 47401.

[1] W. R. Hess, Phys. Rev. A 9, 2036 (1974).

[2] E. W. Thomas, *Excitation in Heavy Particle Collisions* (Wiley, New York, 1972).

[3] R. H. Hughes, C. A. Stigers, B. M. Doughty, and E. D. Stokes, Phys. Rev. A 1, 1424 (1970).

[4] J. C. Ford and E. W. Thomas, Phys. Rev. A 5, 1701 (1972).

[5] S. H. Neff, private communication.

[6] S. H. Neff, Astrophys. J. 140, 348 (1964).

[7] S. H. Neff, Astrophys. J. 170, 235 (1972).

[8] D. F. Collins, B. Q. McGimsey, and R. C. Isler, Bull. Am. Phys. Soc. 16, 1342 (1971), and private commun-

ication.

[9]J. Weiner, Ph.D. dissertation (The University of Chicago, 1970) (unpublished).

[10]J. Weiner, W. B. Peatman, and R. S. Berry, Phys. Rev. A $\underline{4}$, 1824 (1971).

[11]B. L. Blaney, Ph.D. dissertation (The University of Chicago, 1975) (unpublished).

[12]S. A. Pollack, Appl. Opt. $\underline{5}$, 1749 (1966).

[13]G. Hass, in *Applied Optics and Optical Engineering, Vol. III*, edited by R. Kingslake (Academic, New York, 1965), p. 309.

[14]G. Hass and J. E. Waylons, J. Opt. Soc. Am. $\underline{51}$, 719 (1961).

[15]E. P. Andreev, V. A. Ankudinov, and S. V. Bobashev, Opt. Spectrosk. $\underline{16}$, 187 (1964) [Opt. Spectrosc. $\underline{16}$, 103 (1964)].

[16]W. L. Wiese, M. W. Smith, and B. M. Glennon, *Atomic Transition Probabilities*, NSRDS-NBS4, Vol. I (U. S. GPO, Washington, D. C., 1966).

[17]Y. B. Band, J. Phys. B $\underline{7}$, 2055 (1974).

[18]J. R. Oppenheimer, Phys. Rev. $\underline{51}$, 349 (1928).

[19]J. D. Jackson and H. Schiff, Phys. Rev. $\underline{89}$, 359 (1952).

[20]D. R. Bates and R. McCarroll, Adv. Phys. $\underline{11}$, 39 (1962).

[21]D. Jaecks, B. Van Zyl, and R. Geballe, Phys. Rev. $\underline{137}$, A340 (1965).

[22]H. H. Harris, M. G. Crowley, and J. J. Leventhal, Phys. Rev. Lett. $\underline{34}$, 67 (1975); (also to be published).

[23]H. R. Dawson and D. H. Loyd, Phys. Rev. A $\underline{9}$, 166 (1974).

[24]R. Stair, W. E. Schneider, and J. K. Jackson, Appl. Opt. $\underline{2}$, 1151 (1963).